ORIGINAL PAPER

Journal of Anatomy   ANATOMICAL SOCIETY WILEY

Anatomical variation of the aorta in the West of Scotland – A population with high cardiovascular disease burden. Implications for stent design and deployment

Hazel Allardyce[1,2] | Ellis Shepherd[1] | Emma L. Bailey[1] 🆔

[1]College of Medicine, Veterinary Medicine, Dentistry and Life Sciences, University of Glasgow, Glasgow, UK

[2]School of Medicine, Medical Sciences & Nutrition, University of Aberdeen, Institute of Medical Sciences, Aberdeen, UK

Correspondence
Emma L. Bailey, College of Medicine, Veterinary Medicine, Dentistry and Life Sciences, University of Glasgow, Glasgow, UK.
Email: emma.bailey@glasgow.ac.uk

Abstract

The prevalence and complexity of cardiovascular disease (CVD) in the West of Scotland are high with the aortic arch and abdominal aorta, particularly at increased risk of cardiovascular pathology. Stent deployment can be key in preventing further cardiovascular events, however, current stent design does not account for complex advanced CVD in these areas. This cadaveric study aimed to provide anatomical measurements requested by manufacturers to improve stent design and deployment in this target population. Nine cadavers (six females and three males; age range = 82.7 ± 10.4 years) from the West of Scotland were dissected to expose the aortic arch and abdominal aorta. Digital callipers and protractors were used to collect data on vessel diameters (including taper), branch spacing, angles and presence of collaterals. CVD was present in all cadavers and ranged from mild plaque presence to aortic dissections. One possessed a bovine aortic arch variation. Supra-aortic vessels were approximately equally spaced, but the left common carotid had the most acute branching angle. Angulation of the arch from the coronal plane positively correlated with a deviation of the left subclavian artery (LSA) from the sternal midline (Spearman's coefficient $r = 0.82$, $p = 0.01$) which may impact surgical access. The origin of the vertebral artery on the LSA was also highly variable. The diameter of the descending aorta decreased along its length from the aortic hiatus to superior mesenteric by $21 \pm 10\%$ indicating a high degree of taper. The artery of Adamkiewicz was present in 33% and additional renal collaterals were present in 22%. 66% had tortuous vessels in the abdominal region. These results highlight the need for more data to aid the refinement of stent-graft design and deployment methods to ensure successful surgical intervention in this population.

KEYWORDS
abdominal aorta, aortic arch, cardiovascular disease, stent

1 | INTRODUCTION

Cardiovascular disease (CVD) is the leading cause of mortality in Scotland, causing 15,000 deaths per year and affecting an estimated 685,000 of the population (BHF, 2021). Over the last decade, increased awareness of causative lifestyle factors has led to a 30% decrease in the prevalence of CVD in the UK, however, the incidence of premature death directly resulting from CVD remains highest in the West of Scotland (Public Health Scotland, 2021). Compared to other regions in Scotland, Glasgow has the highest fatality rate for premature heart and circulatory disease (BHF, 2021). The "Glasgow Effect" is the increased likelihood of death before aged 65, and while lifestyle choices including smoking, physical inactivity and poor diet are associated, this phenomenon shows no socio-economic disparity (Cowley et al., 2016). This group also suffers from a greater variety of complex CVD which requires more challenging and/or repeated clinical interventions (Public Health Scotland, 2021).

Cardiovascular disease is commonly the result of chronic atherosclerosis, manifestations of which frequently form in areas of complex vascular geometry with turbulent blood flow. With high degrees of curvature and/or with several vessel bifurcations, the aortic arch and abdominal aorta are associated with an increased risk of plaque formation and vessel weakness (Assemat et al., 2014). To control susceptibility to serious cardiovascular events, such as aortic dissection or aneurysm rupture, early clinical intervention is key. Routinely, stent-grafts are utilised to maintain the integrity of a diseased arterial wall, redirecting blood flow and preventing rupture of aneurysms (Peters et al., 2009). Stent-graft development has advanced dramatically since overtaking balloon angioplasty as the most effective interventional therapy, however, due to the complex geometry and other confounding factors like blood flow profiles, the design of stent-grafts for the arch and abdominal aorta is challenging.

A high degree of anatomical variation is recognised in the healthy aorta (Popieluszko et al., 2017), thought to be the result of its complex embryonic development – curvature and angulation of the arch can vary, as well as origin and angulation of the supra-aortic vessels (Hanneman et al., 2017). Some variation is important to know not for design but for deployment – for example the left subclavian artery (LSA) is the deepest in the thorax and furthest from the initial surgical incision so variation in its position can influence catheter choice. The abdominal aorta also shows variation in the origin and course of its principal branches, with approximately 40% displaying differing configurations (Kornafel et al., 2010). Stent-graft design is currently based on MRI imaging of relatively healthy individuals; however, it is likely that such configurations do not reflect the aortic anatomy of the target population with diagnosed CVD. CVD can cause remodelling including changes in vessel diameters, increased tortuosity and blockages due to plaque.

The complexity of the CVD often results in several and extensive disease sites which require an integrated hybrid stent-graft with the capacity to treat more than one branch in a single surgery. To enable successful deployment and function, grafts must account for branching patterns, branch diameters, locations and angulation of

vessels to ensure alignment of often multiple branching arms. For aortic arch stents, knowledge of the origin of the vertebral artery on the LSA is also vital as occlusion may lead to oxygen starvation of the posterior cerebrum. Similarly, in the abdomen the presence and/or occlusion of the artery of Adamkiewicz can impact spinal tissue perfusion. These types of measurement are not currently well characterised in the target population and more data is required to inform the design and surgical deployment of devices in these anatomical areas.

Therefore, the aim of this study was to acquire pertinent measurements in a West of Scotland cadaveric cohort to assist in the refinement of complex vascular prosthetic design and inform surgical deployment in the target population.

2 | METHODS

Data was collected from nine formalin-fixed cadavers (six females and three males; age range $= 82.7 \pm 10.4$ years) from the West of Scotland. Ethical approval for this study was provided by the University of Glasgow and was conducted in accordance with the Anatomy Act (1984), and Human Tissue Act (Scotland) 2006. Standard dissection protocols based on Cunninghams (Cunningham, 1986) were utilised to expose the aortic arch and abdominal aorta. Skin, adipose tissue, superficial fascia and musculature from the upper mediastinum, thorax and abdomen were reflected laterally or removed. Ribs were disarticulated at the midaxillary line and clavicles were dislocated at the point of anterior scalene. The chest wall was mobilised with clavicles attached and the internal thorax exposed. Lungs and pericardium were removed to expose heart walls. The superior vena cava and brachiocephalic veins were removed to expose the aortic arch and supra-aortic branches. Abdominal viscera were removed with exception of the urogenital organs to expose the abdominal aorta. The following vessels were identified; the coeliac trunk, superior mesenteric artery (SMA), renal arteries, inferior mesenteric artery (IMA) and the bifurcation of the aorta into the iliac arteries.

2.1 | Data collection

The following measurements were taken following consultation with stent design engineers from Terumo Aortic Limited – a company based in the West of Scotland that designs highly complex devices for complex CVD patients and who work closely with cardiothoracic surgeons to optimise their deployment.

2.2 | Aortic arch

The type of aortic arch branching pattern was determined by referencing published literature (Lale et al., 2014). External vessel diameters were measured using digital callipers at the point of vessel origin for the brachiocephalic trunk (BCT), left common carotid (LCC) and LSA.

Distance between the supra-aortic vessels was measured by pinning the midpoint of the BCT, LCC and LSA then digital callipers measured the distance between. The total distance between the BCT and LSA was calculated by the addition of the two previous values. Arch angulation (from the coronal plane) was determined using a modified published method (O'Malley et al., 2018). The most prominent point to the left of the origin of the ascending and descending aorta was pinned. A piece of string was passed from the descending aorta to the pin on the ascending and then across a coronal plane extended to the left side of the cadaver (Figure 1a). A protractor was used to acquire the angle between the coronal plane and the aorta. Distance between the sternum and LSA: the chest wall was rearticulated onto the thorax and midpoint of sternum was pinned at the level of the second rib to recreate surgical access via a median sternotomy. The LSA was pinned at its origin from the arch. String was extended from the midline of the sternum in a lateral direction to form a horizontal plane and from the origin of the LSA in a vertical plane to form a right-angle with the horizontal plane (deviation of LSA to left of the midline of the thorax). Pythagoras' theorem was used to calculate the length of the hypotenuse, and therefore the distance between sternum and LSA (Figure 1b). This method was used to reduce user bias in simply using digital callipers. Angulation of supra-aortic vessels was determined by placing a protractor along the axis of the aortic arch and the angle between the aorta and the left wall of the branching vessel was recorded (Figure 1c).
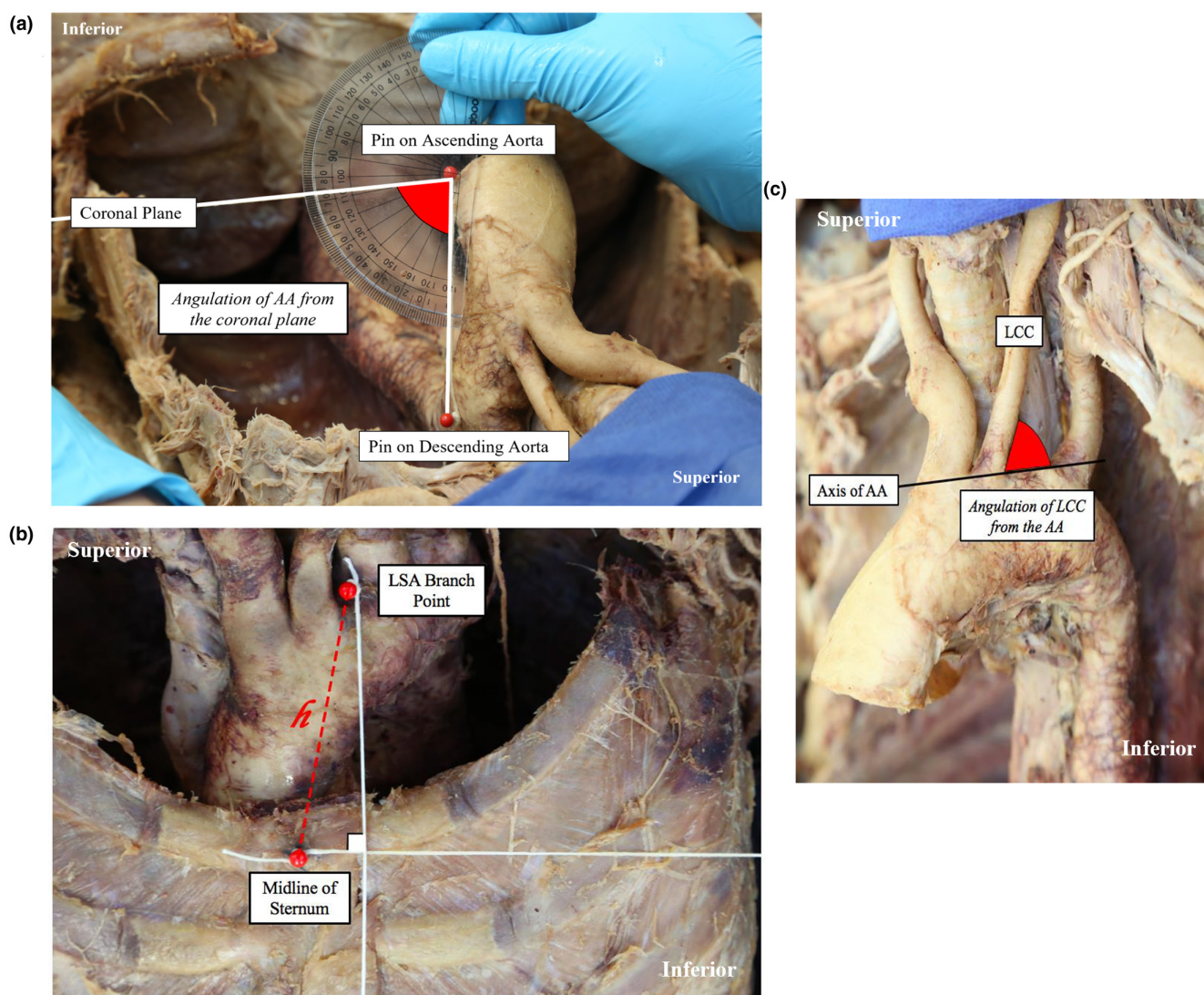

FIGURE 1 (a) Measurement of angulation of the aortic arch from the coronal plane. Pins are placed in the most prominent points at the left side of the origin of the ascending and descending aorta. String extended between these points and across to form a coronal plane. Angle determined using a protractor. (b) Distance from sternal midline at level of the second rib to the origin of the left subclavian artery (LSA) on the aortic arch (AA) using Pythagorean theorem. Each point pinned with string extended from the sternum in a horizontal plane and from the LSA in a vertical plane to form a right-angle. The hypotenuse; distance between the pinned points, was calculated using function $a2 + b2 = c2$. (c) Angulation of each branching vessel from the AA is determined by placing a protractor along the axis of the AA and deducing the angle between the axis and left-sided wall of each vessel. Image depicts an example of the measurement of LCC angulation. Black line is the axis of the AA, with red shaded area the angle measured

2.3 | Abdominal aorta

Measurements included diameter of the aorta at the level of the aortic hiatus (AH) and SMA, principal branch diameters, angles, distances from branch to branch, and from the AH. Again, measurements were taken using Digital Callipers and protractors. The renal arteries were not included in angle measurements due to their tortuous nature making accurate measurement too difficult. Lumbar arteries were identified and counted bilaterally in addition to any arteries of collateral flow, namely the artery of Adamkiewicz. Incidental findings were noted including aneurysms, dilations and tortuous vessels. The presence of atherosclerotic plaques and/or calcification of vessel walls was also noted.

2.4 | Data analysis

All statistical testing was undertaken using GraphPad Prism 8 software. All results are reported as mean ± standard deviation unless stated otherwise. Statistical significance is reported where * denotes $p < 0.05$, ** $p < 0.01$ and *** $p < 0.001$. Aortic Arch Data – For spacing of supra-aortic branching, statistical significance was calculated using the Mann–Whitney U-test. For branching angulation, outliers were determined using Grubb's outlier test and removed before further analysis. Statistical significance was calculated using the Kruskal–Wallis ANOVA with Dunn's multiple comparison post hoc test. Spearman's rank correlation was implemented to determine the associations between arch angulation, distance between sternal midline and LSA, and deviation of LSA to left of the midline.

Abdominal Data – Differences in the diameter of the aorta, from the AH to the point of the SMA were calculated as a percentage change. Diameters of the principal abdominal branches were analysed using paired T-tests and ranked in order of size (from 1 to 5) for each cadaver; where an observed ranking based on the mode of their diameters was established and compared to data from literature as an expected rank.

3 | RESULTS

3.1 | Incidence and type of CVD

CVD pathology was noted in all individuals and specifically recorded in 8/9 cadavers reflecting the high CVD prevalence in the West of Scotland. Ischaemic heart disease, myocardial infarction, stroke and congestive heart failure were just some of the cardiovascular conditions recorded at death (Table S1). At least three of the cadavers presented with calcified atherosclerotic plaques. Two individuals also had severe aortic dissections even though they were not listed as the cause of death. One of these aortic dissections was extensive, advancing from the ascending aorta through all branches and along distal descending aorta.

3.2 | Measurements of the aortic arch

3.2.1 | Branching pattern, diameter, spacing and angulation of the supra-aortic branches

Of the nine cadavers investigated, eight (89%) had the normal arch branching configuration; separate BCT, LCC and LSA branches. One (11%) was found to have the bovine variation, with a common origin of the BCT and LCC, and a separate LSA branch. External diameter of the BCT was 13.63± 2.61 mm, LCC 8.06 + 1.84 mm and LSA 12.21 + 3.45 mm. Previous literature has reported a range of 8.3–15.5 mm for the BCT, 4.6–7.4 mm for the LCC and 6–12.8 mm for the LSA (Kahraman et al., 2006; Manole et al., 2013), therefore whilst our values were at the upper end of these ranges or slightly larger in the case of the LCC they generally reflect previous findings. The proximity of the supra-aortic branches showed the mean distance between the midpoint of the BCT-LCC as 18.2 ± 3.3 mm, and between the LCC-LSA as 19.6 ± 5.3 mm. No significant difference was determined between BCT-LCC and LCC-LSA ($p = 0.54$), suggesting approximately equal spacing of the branches along the arch. Distance between the BCT-LSA was calculated as 37.8 ± 6.3 mm. Branching angle of the supra-aortic vessels from smallest to largest, respectively, was LCC (59° ± 26), BCT (70° ± 26) and LSA (75° ± 15). A significant difference was determined only between branching angle of LCC and LSA ($p = 0.02$). All measurements showed a large minimum to maximum range, highlighting a high degree of inter-individual variation. All measurements showed a large minimum to maximum range, highlighting a high degree of inter-individual variation (Table S2).

3.2.2 | Relationship between LSA, aortic arch and sternal midline

Mean angulation of the aortic arch (AA) from the coronal plane was found to be 64° ± 14, (range 39–86°). Distance between the sternal midline and the emergence of LSA on the arch was calculated as 84.6 ± 14.1 mm, (range 67.21–108.4 mm). Mean deviation of LSA to the left of the midline was 24.9 mm ± 11.85, (range 6.0–48.1 mm). Angulation of the aortic arch and the distance from the sternal midline to the emergence of the LSA was found to be positively correlated but not significant ($r = 0.48$, $p = 0.19$). A significant positive correlation was, however, determined between AA angulation and deviation of LSA from the sternal midline ($r = 0.82$, $p = 0.01$) (Figure 2).

3.2.3 | Origin of the vertebral artery

Mean distance from the origin of the LSA to the emergence of the left vertebral artery was 33.7 ± 6.8 mm (range 23.8–46.5 mm) and the external diameter of the left vertebral artery was 4.9 ± 0.8 mm (range 3.6–6.2 mm). Only a weak positive correlation ($r = 0.2$,
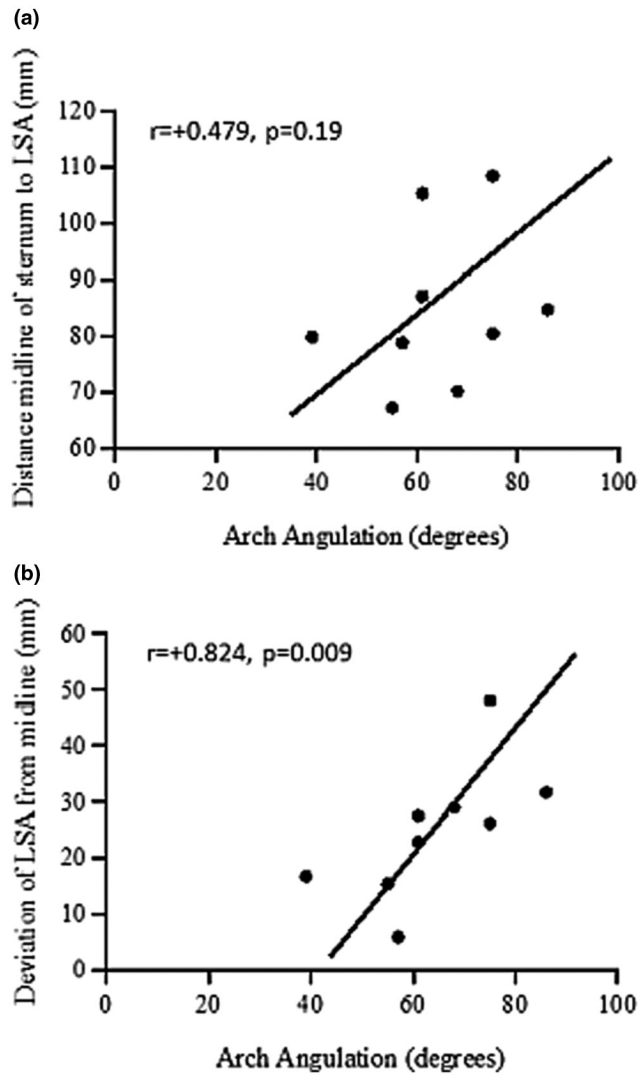
(a)

(b)

FIGURE 2 Spearman's rank coefficient was utilised to determine if a positive correlation existed between variables. (a) A positive trend correlation was revealed between angulation of arch and distance between midline of the sternum to the left subclavian artery (LSA), however, results were not significant ($r = +0.48$, $p = 0.19$). (b) A statistically significant positive correlation was determined between angulation of arch and deviation of LSA to the left from the sternal midline ($r = +0.82$, $p^{**} = 0.01$), $n = 9$

$p = 0.59$) was evident between point of origin of vertebral artery on the LSA and external diameter.

3.3 | Measurements of the abdominal aorta

3.3.1 | Principal branch diameters and their rank position

From superior to inferior the mean diameters of the principle branches were as follows: Coeliac 5.7 ± 1.7 mm, SMA 8.1 ± 2.7 mm, IMA 2.4 ± 0.6 mm, Left Renal 5.5 ± 1.3 mm and Right Renal 5.5 ± 1.1 mm. Previous studies found branch mean diameters

of the coeliac trunk, SMA and IMA to be 6 ± 1.6, 7.8 ± 1.7 and 3.6 ± 0.7 mm respectively with the left and right renals at 5.2 ± 1.4 and 4.9 ± 1.2 mm (Schonherr et al., 2016; Songür et al., 2010). *T*-test analysis of these figures showed that only the IMA was significantly smaller in our cohort ($p < 0.001$). The IMA was consistently the smallest vessel whilst the coeliac artery showed the most variability in rank position. The SMA was predominantly the largest branch when ranked, however, there was an outlier in cadaver 6 where the left renal had the largest diameter. Observed versus expected rank in general was consistent with the literature except for the left and right renal arteries which swapped positions (Table S3) with the left ranking higher than the right.

3.3.2 | Aortic diameter significantly decreases with distance from the AH

The diameter of the aorta from the AH to the SMA decreased in 8/9 cadavers and actually increased in one indicating a probable aneurysm. Excluding this cadaver, the mean diameter at the AH was 27.4 ± 8.1 mm and at the SMA was 21.3 ± 6.0 mm and resulted in an average percentage decrease of $21.5 \pm 10.3\%$.

3.3.3 | Presence of collateral vessels and tortuous branches (Figure 3)

The presence of collateral and tortuous branches were calculated as a percentage of the sample population. 3/9 (33.3%) cadavers displayed a potential artery of Adamkiewicz, and 2/9 (22.2%) possessed at least one additional renal artery. Collateral vessels were found where aortas had a high incidence of plaque. 66.6% of cadavers displayed tortuous vessels, of this 33.3% of the tortuous vessels were collaterals.

4 | DISCUSSION

This study sought to provide pertinent measurements requested by a stent manufacturer in the target population to improve both design and deployment of these complex devices. In the aortic arch, supra-aortic branch configuration and spacing did not differ from normal. Location of the supra-aortic vessel origins and angulation of the arch itself from the coronal plane showed high inter-individual variation in agreement with previous studies. Diameters of the supra-aortic branches whilst at the higher end of previously reported ranges were not significantly larger. This study, however, has shown that in this population high angulation of the arch from the coronal plane was positively correlated with deviation of LSA from the sternal midline which may impact surgical access to the target site. We also show the origin of the vertebral artery on the LSA to be highly variable therefore the length of the LSA arm on an arch device should take this into account to prevent potential vertebral artery obstruction. In
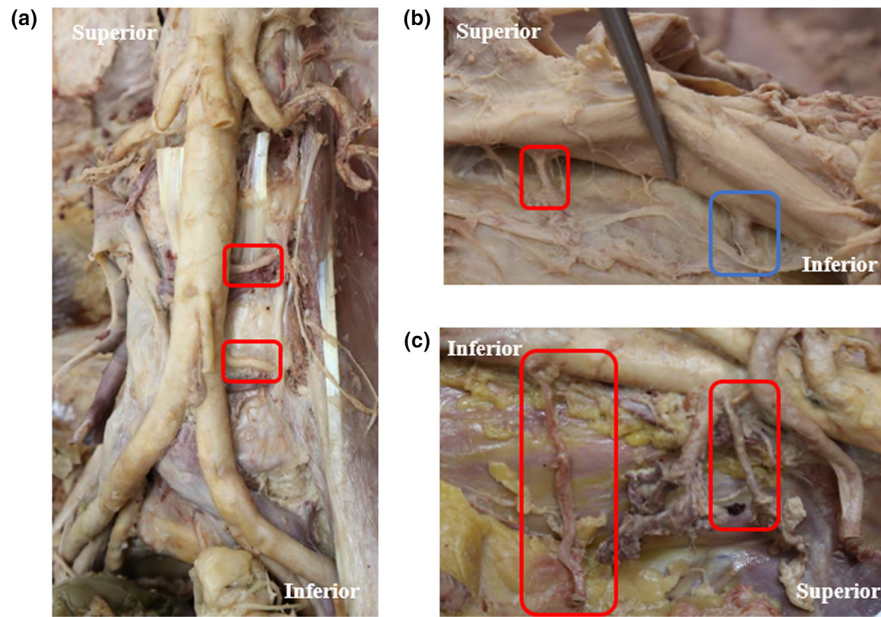
FIGURE 3 (a) A dissection of the abdominal aorta with two lumbar arteries highlighted by red boxes. (b) A section of the abdominal aorta is shown with a lumbar artery highlighted by a red box, a potential artery of Adamkiewicz is highlighted by the blue box as evidenced by the increased vessel diameter and direction of the vessel as it continues into the spinal muscles. (c) A section of dissected abdominal aorta with collateral flow renal vessels is highlighted by red boxes. The left collateral vessel is slightly tortuous. The renal artery is evident between

the abdominal aorta our study found a high degree of taper and incidence of both extra collaterals and/or tortuous branches – factors which can influence both fit and deployment in this region. Sizeable variation in principle branch diameters was also evident and the left renal was more often larger in diameter than the right – in contrast to previous literature. Consequently, device manufacturers can do more to tailor their devices to the target population and ensure better surgical success.

4.1 | Implications for aortic arch stents

Stents designed for the aortic arch should consider branching pattern, vessel diameters, location of vessel origins and angulation of vessels. In this cohort, we report typical branching pattern in 89% of individuals, with one incidence of the bovine variant, in agreement with previous literature (Jalali Kondori et al., 2016; Karacan et al., 2014; O'Malley et al., 2018; Patil et al., 2012). Based on these findings, a stent-graft design of the most common anatomical configuration would be applicable to majority, however, alternative stent-graft models are required for use in cases of anatomical variation, with preoperative imaging to determine arch morphology. Branching angulation of the supra-aortic vessels is likely determined by developmental origins and location of the aortic arch in the thorax due to the course they follow into the superior mediastinum, however, there is very little literature to provide reasoning for the variability in branching angles of these vessels from the arch that we have described. Branch diameters were either at the upper end of previously reported ranges (BCT & LSA) or slightly larger (LCC), however, not to a significant degree. The flexible material of most stents would account for this slight dilation in our population

which is likely a combined result of age and disease presence. These results highlight the need for a range of stent-graft models with differing proximity of branching arms or ideally custom-made devices, as a standard model is unlikely to fit the requirements of a population. Careful consideration should also be taken in the design of length of branching arms as occlusion of the vertebral artery, the first branch of the LSA, may result in hypoxic injury of the posterior cerebrum. It is also worth noting that the vertebral artery itself can arise directly from the arch (Onrat et al., 2021) and although we did not encounter this variant it may also hinder the deployment and placement of a stent-graft in this area.

We have shown angulation of the arch to be highly variable between individuals, ranging between 39–86° in this cohort, with similar reports in an Irish population, between 25° and 76°, (O'Malley et al., 2018) and the Korean population, ranging 30°–90° (Shin et al., 2008). A higher degree of angulation would require a longer length of the catheter for successful stent delivery. Location of the LSA can also pose challenges during surgery as it is the farthest from the surgical incision point of a median sternotomy. We show further variation in distance between the sternal midline and the origin of the LSA and furthermore, high angulation of the arch from the coronal plane was positively correlated with deviation of LSA from the sternal midline. This is likely influenced by the geometry of the aortic arch in 3D space and by surrounding structures such as the trachea, oesophagus and spinal column that limit its rotation during development. A higher angulation would cause a shift of the entire arch to the left side of the body, resulting in an increased deviation to the left of all branching vessels from the sternal midline and therefore increased distance from the incision of a median sternotomy. Finally, the presence of not one but two aortic dissections in our

small cohort raise the question as to whether this may be a more common occurrence in this population and should be actively looked for on any pre-operative imaging.

4.2 | Implications for abdominal aortic stents

Incorporating visceral arteries into prostheses design has become increasingly popular, with several branches and arterial attachments on stent-grafts shown to result in lower occlusion rates. However, due to the use of standardised measurements as a design tool, graft detachment and endoleaks (blood diversion between the graft and artery wall) are common (Mendes & Oderich, 2016). As each abdominal organ has its own demand for blood delivery, branches of the aorta are normally of varying diameters, however, pathology of CVD can further complicate matters by altering the normal morphology. In this cohort only the IMA was found to be significantly different from previous literature (Songür et al., 2010) presenting as ~1 mm smaller than average, however, our small cohort size and /or older aged cohort may explain this and more data in a severe CVD population would be needed to infer any CVD involvement. We also report variation in the ranking of the principle abdominal branches which is concurrent with previous literature that indicates a "one size fits all" stent is not an optimal design to ensure surgical success (Sweet et al., 2009; Watson et al., 2017).

The abdominal aorta shows a degree of taper in a cranial-caudal direction. This is important in the context of haemodynamics and the fit of any device, as a stent-graft should be flush against the vessel lumen. Stent-graft constructs have a limited capacity to stretch and therefore if fit is insufficient, can result in endoleak and collapse of the device, a common complication of endovascular aneurysm repair (Daye & Walker, 2018). This study cohort showed a 21% average decrease from the AH to the SMA. Whilst a degree of taper is attributed to the decrease in blood volume as it disperses to the abdominal viscera, age and sex are also known to have effects (Pennington & Soames, 2005). In a population, aged 19–67, an average decrease of ~12% for men and ~17% for women between the coeliac trunk and inter-renal segments was reported, with increased taper in advancing age, particularly pronounced in the infra-renal segment (Fleischmann et al., 2001). Vessel taper may predispose and/or exacerbate CVD due to turbulent vortical flow in the aorta, influencing shear stress on the vessel wall (Peiffer et al., 2012). Pathogenesis of both atherosclerosis and aortic aneurysms have been attributed to abnormalities in blood flow, shear stress and wall strain (Pennington & Soames, 2005) – all influenced by taper (Knobelsdorff-Brenkenhoff et al., 2016).

Torturous vessels, with kinked, twisted or curled morphology, were present in 66.6% of this cohort. Vessels affected included renal arteries, coeliac trunk, SMA and collateral vessels. Such torturous branches may develop from hypertension, occlusion of local vessels, atherosclerotic lesions or during development. Whilst mild, tortuous arteries are usually asymptomatic, severe torsion can result in ischaemia downstream (Han, 2012). They can also be difficult

to manoeuvre as, without prior imaging, a straight tipped catheter or endovascular balloon may puncture the vessel (Kara et al., 2011). The artery of Adamkiewicz is critical in providing alternative flow to the anterior part of the lumbar and sacral spinal cord and is present in 84.6% of the population (Taterra et al., 2019). Its presence can be problematic when designing an optimal stent-graft as occlusion by a multi-branched construct may result in decreased spinal perfusion, leading to post-operative lower extremity weakness, paraparesis and paraplegia (Mutch & Johansson, 2011). Collateral vessel formation may be the result of haemodynamic forces that increase shear stress on the vessel wall but are of higher prevalence in individuals with CVD risk factors (De Groot et al., 2009). In cases of CVD, additional collateral vessels may develop in highly diseased areas to bypass obstructions (e.g. atherosclerotic plaques) and preserve tissue from ischaemia. Collateral renal, adrenal, lumbar, peri-ureteric and intra-renal arteries are often reported in severe CVD cases (Hardman et al., 2011) so it is unsurprising to find extra collateral vessels in this cohort.

4.3 | Study limitations

This study should be considered as pilot data due to the small cohort included, however, the presence of CVD pathology was high and accurately reflected the West of Scotland population. Future work would increase cohort size and investigate more males to reflect disease prevalence. Cadaveric studies have innate limitations such as shrinkage of material during the embalming process. This would occur in all cadavers to the same extent and so comparison between individuals remains accurate, however, when comparing to patient data this difference should be acknowledged. It must also be noted that during surgical procedures both the heart and branching vessels are under control of and reflect the heartbeat, and so vascular dynamics would impact vessel geometry in vivo (Shin et al., 2008) which a cadaveric study cannot account for. Future work should consider combining imaging techniques and 3D photogrammetry to reconstruct the AA and surrounding structures digitally, improving the accuracy of angular measurements. Whilst imaging can provide ways around some of these limitations, data from cadaveric studies remains valuable in providing measurements important to obtain from pre-operative imaging, which should be included in clinical practice for all complex CVD patients due to receiving a device.

4.4 | Considerations for future stent design and deployment

As incidence of CVD is extremely high in the West of Scotland, knowledge of the true anatomy of the aorta is required to guide design and development of optimal prostheses for surgical intervention. This pilot study is the first to characterise anatomical variation of the aorta within this cohort and shows that the "normal" anatomy, from which stent-grafts have been designed until now,

is not reflective of what exists. Whether by anatomical variation or confounding effects of CVD, high inter-individual variation has been described in all aspects of the aorta investigated. These data highlight the need for further study to aid in the refinement of stent-graft design and deployment methods to ensure successful surgical intervention.

AUTHOR CONTRIBUTIONS

Ellis Shepherd performed dissection, acquired measurements, analysed data, drafted and edited the manuscript. Hazel Allardyce performed dissection, acquired measurements, analysed data, drafted and edited the manuscript. Emma L. Bailey conceived the study, drafted, edited and critically analysed the manuscript.

DATA AVAILABILITY STATEMENT

Data available in article supplementary material. The data that supports the findings of this study are available in the supplementary material of this article.

ORCID

Emma L. Bailey https://orcid.org/0000-0003-3826-9956

REFERENCES

Assemat, P., Siu, K.K., Armitage, J.A., Hokke, S.N., Dart, A., Chin-Dusting, J. et al. (2014) Haemodynamical stress in mouse aortic arch with atherosclerotic plaques: preliminary study of plaque progression. *Comput Struct Biotechnol J*, 10, 98–106.

BHF. 2021. *Heart and circulatory disease statistics 2021* [Online]. https://www.bhf.org.uk/what-we-do/our-research/heart-statistics/heart-statistics-publications/cardiovascular-disease-statistics-2021.

Cowley, J., Kiely, J. & Collins, D. (2016) Unravelling the Glasgow effect: the relationship between accumulative bio- psychosocial stress, stress reactivity and Scotland's health problems. *Prev Med Rep*, 4, 370–375.

Cunningham, D.J.R.G.J. (1986) *Cunningham's manual of practical anatomy*, Vol. 2. Oxford: Oxford University Press.

Daye, D. & Walker, T.G. (2018) Complications of endovascular aneurysm repair of the thoracic and abdominal aorta: evaluation and management. *Cardiovasc Diagn Ther*, 8(Suppl 1), S138–S156.

De Groot, D., Pasterkamp, G. & Hoefer, I.E. (2009) Cardiovascular risk factors and collateral artery formation. *Eur J Clin Investig*, 39, 1036–1047.

Fleischmann, D., Hastie, T.J., Dannegger, F.C., Paik, D.S., Tillich, M., Zarins, C.K. et al. (2001) Quantitative determination of age-related geometric changes in the normal abdominal aorta. *J Vasc Surg*, 33, 97–105.

Han, H.C. (2012) Twisted blood vessels: symptoms, etiology and biomechanical mechanisms. *J Vasc Res*, 49, 185–197.

Hanneman, K., Newman, B. & Chan, F. (2017) Congenital variants and anomalies of the aortic arch. *Radiographics*, 37, 32–51.

Hardman, R.L., Lopera, J.E., Cardan, R.A., Trimmer, C.K. & Josephs, S.C. (2011) Common and rare collateral pathways in aortoiliac occlusive disease: a pictorial essay. *Am J Roentgenol*, 197, W519–W524.

Jalali Kondori, B., Asadi, M.H.Ossei, Rahimian, E. & Tahsini, M.R. (2016) Anatomical variations in aortic arch branching pattern. *Arch Iran Med*, 19, 72–74. https://pubmed.ncbi.nlm.nih.gov/26702752/

Kahraman, H., Ozaydin, M., Varol, E., Aslan, S.M., Dogan, A., Altinbas, A. et al. (2006) The diameters of the aorta and its major branches in patients with isolated coronary artery ectasia. *Tex Heart Inst J*, 33, 463–468.

Kara, E., Celebi, B., Yildiz, A., Ozturk, N. & Uzmansel, D. (2011) An unusual case of a tortuous abdominal aorta with a common celiacomesenteric trunk: demonstrated by angiography. *Clinics*, 66, 169–171.

Karacan, A., Türkvatan, A. & Karacan, K. (2014) Anatomical variations of aortic arch branching: Evaluation with computed tomographic angiography. *Cardiol Young*, 24, 485–493.

Knobelsdorff-Brenkenhoff, F.V., Karunaharamoorthy, A., Trauzeddel, R.F., Barker, A.J., Blaszczyk, E., Markl, M. et al. (2016) Evaluation of aortic blood flow and wall shear stress in aortic stenosis and its association with left ventricular remodeling. *Circ Cardiovasc Imaging*, 9, e004038.

Kornafel, O., Baran, B., Pawlikowska, I., Laszczyński, P., Guziński, M. & Sąsiadek, M. (2010) Analysis of anatomical variations of the main arteries branching from the abdominal aorta, with 64-detector computed tomography. *Pol J Radiol*, 75, 38–45.

Lale, P., Toprak, U., Yagiz, G., Kaya, T. & Uyanik, S.A. (2014) Variations in the branching pattern of the aortic arch detected with computerized tomography angiography. *Adv Radiol*, 2014, 969728.

Manole, A.M., Iliescu, D., Rusali, L. & Bordei, P. (2013) Morphometry of the aortic arch and its branches. *ARS Medica Tomitana*, 19, 154–159.

Mendes, B.C. & Oderich, G.S. (2016) Endovascular repair of thoracoabdominal aortic aneurysm using the off-the-shelf multibranched t-branch stent graft. *J Vasc Surg*, 63, 1394–1399.e2.

Mutch, J.A.J. & Johansson, J.E. (2011) Occlusion of the artery of Adamkiewicz after hip and knee arthroplasty. *J Arthroplast*, 26, 505.e5–505.e8.

O'Malley, A.M., El Kininy, W.H., Debebe, H., Burukan, A.B. & Davy, S.W. (2018) A cadaveric study of aortic arch variation in an Irish population. *Ir J Med Sci (1971)*, 187, 853–858.

Onrat, E., Uluişik, I.E. & Ortug, G. (2021) The left vertebral artery arising directly from the aortic arch. *Transl Res Anat*, 24, 100122.

Patil, S.T., Meshram, M.M., Kamdi, N.Y., Kasote, A.P. & Parchand, M.P. (2012) Study on branching pattern of aortic arch in Indian. *Anat Cell Biol*, 45, 203.

Peiffer, V., Rowland, E.M., Cremers, S.G., Weinberg, P.D. & Sherwin, S.J. (2012) Effect of aortic taper on patterns of blood flow and wall shear stress in rabbits: association with age. *Atherosclerosis*, 223, 114–121.

Pennington, N. & Soames, R.W. (2005) The anterior visceral branches of the abdominal aorta and their relationship to the renal arteries. *Surg Radiol Anat*, 27, 395–403.

Peters, B., Ewert, P. & Berger, F. (2009) The role of stents in the treatment of congenital heart disease: current status and future perspectives. *Ann Pediatr Cardiol*, 2, 3–23.

Popieluszko, P., Henry, B., Sanna, B., Hsieh, W.C., Saganiak, K., Pękala, P. et al. (2017) A systematic review and meta-analysis of variations in branching patterns of the adult aortic arch. *J Vasc Surg*, 68, 298–306.

Public Health Scotland. 2021. *Heart disease: Public Health Scotland* [Online]. https://www.isdscotland.org/Health-Topics/Heart-Disease/.

Schönherr, E., Rehwald, R., Nasseri, P., Luger, A.K., Grams, A.E., Kerschbaum, J., et al. (2016) Retrospective morphometric study of the suitability of renal arteries for renal denervation according to the Symplicity HTN2 trial criteria. *BMJ Open*, 6(1), e009351.

Shin, I.Y., Chung, Y.G., Shin, W.H., Im, S.B., Hwang, S.C. & Kim, B.T. (2008) A morphometric study on cadaveric aortic arch and its major branches in 25 Korean adults: the perspective of endovascular surgery. *J Korean Neurosurg Soc*, 44, 78–83.

Songür, A., Toktas, M., Alkoç, O., Acar, T., Uzun, I., Baş, O. et al. (2010) Abdominal aorta and its branches: morphometry—variations in autopsy cases. *Eur J Gen Med*, 7, 321–325.

Sweet, M.P., Hiramoto, J.S., Park, K.-H., Reilly, L.M. & Chuter, T.A.M. (2009) A standardized multi-branched thoracoabdominal stent-graft for endovascular aneurysm repair. *J Endovasc Ther*, 16, 359–364.

Taterra, D., Skinningsrud, B., Pękala, P.A., Hsieh, W.C., Cirocchi, R., Walocha, J.A. et al. (2019) Artery of Adamkiewicz: a meta-analysis of anatomical characteristics. *Neuroradiology*, 61, 869–880.

Watson, T., Webster, M.W.I., Ormiston, J.A., Ruygrok, P.N. & Stewart, J.T. (2017) Long and short of optimal stent design. *Open Heart*, 4, e000680.

SUPPORTING INFORMATION

Additional supporting information may be found in the online version of the article at the publisher's website.

How to cite this article: Allardyce, H., Shepherd, E. & Bailey, E.L. (2023) Anatomical variation of the aorta in the West of Scotland – A population with high cardiovascular disease burden. Implications for stent design and deployment. *Journal of Anatomy*, 242, 112–120. Available from: https://doi.org/10.1111/joa.13652